

# Anharmonicity, mode-coupling and entropy in a fluctuating native protein

A. Kabakcıoğlu<sup>†</sup>, D. Yuret<sup>\*</sup>, M. Gür<sup>\*</sup>, B. Erman<sup>\*</sup>

Colleges of Sciences<sup>†</sup> and Engineering<sup>\*</sup>, Koç University, Sarıyer, 34450, İstanbul, Turkey

E-mail: akabakcioglu@ku.edu.tr

**Abstract.** We develop a general framework for the analysis of residue fluctuations that simultaneously incorporates anharmonicity and mode-coupling in a unified formalism. We show that both deviations from the Gaussian model are important for modeling the multidimensional energy landscape of the protein Crambin (1EJG) in the vicinity of its native state. The effect of anharmonicity and mode-coupling on the fluctuational entropy is on the order of a few percent.

PACS numbers: 87.14.E-, 87.15.-V, 87.85.J-

*Keywords:* protein dynamics, anharmonicity, mode coupling

Submitted to: *Phys. Biol.*

## 1. Introduction

Residue fluctuations of a protein around its native state reveal information that bridges the molecule’s structural and functional properties. At the lowest order, these fluctuations can be treated as a collection of independent harmonic modes, yielding “Elastic Network Models” [1, 2]. On the other hand, it is known that the slowest oscillatory modes of a protein are strongly anharmonic [3, 4, 5], in contrast with the assumption underlying ENMs. The coupling between different modes is another aspect of protein dynamics that is believed to be relevant for the information/energy transfer between different parts of the molecule [6, 7] and not captured by the harmonicity assumption. Our aim here is to gauge respectively the relative contributions of these two distinct anharmonic corrections to the free energy by means of a formalism that distinguishes them naturally.

## 2. Modal expansion and beyond

Sampling the time evolution of a protein by using molecular dynamics reveals a multivariate probability distribution function (pdf)  $f(\Delta\mathbf{R})$  for the deviations of atoms (assume there are  $N$  of them) from equilibrium coordinates, i.e.  $\Delta R_i = R_i - R_i^{eq}$ ,  $i = 1, \dots, 3N$ . We here adopt a coarse-grained representation of this pdf where only  $C^\alpha$  atoms are considered, so that  $N$  is also the number of residues. Accordingly,  $R_i^{eq}$  are the mean  $C^\alpha$  coordinates corresponding to the average configuration of the protein during the part of the trajectory that is used for the calculations.

### 2.1. Hermite expansion

Since the deviations from this free energy minimum are expected to be harmonic for sufficiently small amplitudes, Hermite polynomials - which are orthogonal *wrt* a Gaussian weight function - constitute a natural basis for representing  $f(\Delta\mathbf{R})$ . First, following Ref. [8, 5], we perform the transformation

$$\Delta\mathbf{r} = \langle \Delta\mathbf{R}\Delta\mathbf{R}^T \rangle^{-1/2} \Delta\mathbf{R} . \quad (1)$$

This diagonalizes the covariance matrix  $\Gamma \equiv \langle \Delta\mathbf{R}\Delta\mathbf{R}^T \rangle$  ( $\langle \cdot \rangle$  represents averaging over the trajectory) and would give the normal modes of the protein if fluctuations were harmonic. Otherwise, the distribution function for  $\{\Delta r_i\}$  in its most general form, can be expressed as [9]

$$f(\Delta\mathbf{r}) = \frac{1}{\sqrt{(2\pi)^{3N}}} e^{-\frac{1}{2} \sum_{i=1}^{3N} \Delta r_i^2} \left[ 1 + \sum_{\nu=3}^{\infty} \mathbf{C}_\nu \cdot \mathbf{H}_\nu(\Delta\mathbf{r}) \right] \quad (2)$$

where  $\mathbf{C}_\nu$  (constant) and  $\mathbf{H}_\nu$  (derived below) are tensors of rank  $\nu$ , and the dot product refers to  $\sum_{ij..k} C_\nu^{ij..k} H_\nu^{ij..k}$ . The fluctuations  $\{\Delta r_i\}$  in this mode space spanned by the eigenvectors of  $\Gamma$  are meanless, i.e.,  $\langle \Delta r_i \rangle = 0$ , and decoupled at the lowest (second) order, i.e.,

$$\langle \Delta r_i^T \Delta r_j \rangle = \delta_{ij} . \quad (3)$$

A purely harmonic model is given by  $\mathbf{C}_\nu = 0$ ,  $\forall \nu$ . Note that, the atomic fluctuations corresponding to a given mode can easily be calculated by setting to zero all the eigenvalues except the one of interest, followed by a back transformation of Eq. (1).

Tensor Hermite polynomials can be obtained by successive differentiation using Rodrigues' formula:

$$H_\nu^{ij..k}(\Delta \mathbf{r}) = \frac{(-1)^\nu}{g(\Delta \mathbf{r})} \nabla^{ij..k} g(\Delta \mathbf{r}). \quad (4)$$

Above,  $g(\mathbf{x}) = (2\pi)^{3N/2} \exp(-\mathbf{x}^2/2)$  is the multidimensional Gaussian distribution and  $\nabla^{ij..k} = \nabla^i \nabla^j \dots \nabla^k$  is the gradient tensor with  $\nabla^i \equiv \partial/\partial x_i$ . The tensor coefficients that appear in  $f(\Delta \mathbf{r})$  follow from the orthogonality relation as

$$\mathbf{C}_\nu = \frac{1}{\nu!} \int_{-\infty}^{\infty} \mathbf{H}_\nu(\mathbf{x}) f(\Delta \mathbf{r}) d\Delta \mathbf{r} = \langle \mathbf{H}_\nu(\Delta \mathbf{r}) \rangle / \nu! \quad (5)$$

Therefore, the problem reduces to obtaining the expectation values of the polynomial tensor elements for the system. At the lowest nonvanishing order they read

$$\begin{aligned} \mathbf{H}_3^{111}(\mathbf{x}) &= x_1^3 - 3x_1 \\ \mathbf{H}_3^{112}(\mathbf{x}) &= x_1^2 x_2 - x_2 = \mathbf{H}_3^{121}(\mathbf{x}) = \mathbf{H}_3^{211}(\mathbf{x}) \\ \mathbf{H}_3^{123}(\mathbf{x}) &= x_1 x_2 x_3 = \mathbf{H}_3^{213}(\mathbf{x}) = \dots \end{aligned} \quad (6)$$

Higher order tensor elements can be calculated using a diagrammatic technique. A graphical representation of  $H_4$  in one and two dimensions is given in Fig.1.

$$\begin{aligned} \mathbf{H}_4^{1111}(\mathbf{x}) &= \begin{bmatrix} \bullet & \bullet \\ \bullet & \bullet \end{bmatrix} - 6x \begin{bmatrix} \bullet & \bullet \\ \bullet & \bullet \end{bmatrix} + 3x \begin{bmatrix} \bullet & \bullet \\ \bullet & \bullet \end{bmatrix} = x_1^4 - 6x_1^2 + 3 \\ \mathbf{H}_4^{1112}(\mathbf{x}) &= \begin{bmatrix} \circ & \bullet \\ \bullet & \bullet \end{bmatrix} - 3x \begin{bmatrix} \circ & \bullet \\ \bullet & \bullet \end{bmatrix} - 3x \begin{bmatrix} \circ & \bullet \\ \bullet & \bullet \end{bmatrix} + 3x \begin{bmatrix} \circ & \bullet \\ \bullet & \bullet \end{bmatrix} = x_1^3 x_2 - 3x_1 x_2 \\ \mathbf{H}_4^{1122}(\mathbf{x}) &= \begin{bmatrix} \circ & \circ \\ \bullet & \bullet \end{bmatrix} - \begin{bmatrix} \circ & \circ \\ \bullet & \bullet \end{bmatrix} - \begin{bmatrix} \circ & \circ \\ \bullet & \bullet \end{bmatrix} - 2x \begin{bmatrix} \circ & \circ \\ \bullet & \bullet \end{bmatrix} + \begin{bmatrix} \circ & \circ \\ \bullet & \bullet \end{bmatrix} + \begin{bmatrix} \circ & \circ \\ \bullet & \bullet \end{bmatrix} \\ &= x_1^2 x_2^2 - x_1^2 - x_2^2 + 1 \end{aligned}$$

**Figure 1.** Graphical representation of  $\mathbf{H}_4(\mathbf{x})$  tensor elements in two dimensions. Terms that vanish by virtue of Eq. (3) are crossed.

The inclusion of mode-coupling necessitates consideration of mixed indices (nondiagonal tensor elements). Here, we focus on the coupling between mode pairs and ignore threesome and higher order mixing, i.e., we consider only the bi-polynomials  $\mathbf{H}_\nu^{i_1 i_2 \dots i_\nu}(\Delta r_k, \Delta r_l)$  with  $i_m \in \{k, l\}$ ,  $k, l = 1, 2, \dots, 3N$ . At first sight, estimating the contribution of mode-coupling even at this lowest level appears to be a formidable task, because the number of distinct expectation values to be extracted from the data grows combinatorially. We show below that, the factorization property of the off-diagonal tensor elements and the orthogonality of the modes at the second order bring a significant reduction in complexity, which we exploit to investigate the impact of anharmonicity and mode-coupling separately on the protein dynamics.

We first observe that, the value of a tensor element  $\mathbf{H}_\nu^{i_1 i_2 \dots i_\nu}(\Delta \mathbf{r})$  does not depend on the order of the indices due to the commutativity of the gradient operator,  $\nabla_k \nabla_l - \nabla_l \nabla_k = 0$ . Therefore,

$$\mathbf{H}_\nu^{i_1 i_2 \dots i_\nu}(\Delta \mathbf{r}) = \mathbf{H}_\nu^p(\Delta r_k, \Delta r_l)$$

where  $p$  is the number of indices equal to  $k$  (and the remaining  $\nu - p$  indices are equal to  $l$ ). The fact that the covariance matrix in the normal basis is diagonal further implies that

$$\mathbf{H}_\nu^p(\Delta \mathbf{r}) = H_p(\Delta r_1) \times H_{\nu-p}(\Delta r_2) \quad (7)$$

as is also evident from the Rodrigues's formula in Eq. (4).

## 2.2. Anharmonicity vs mode-coupling

Combining Eq. (5) and Eq. (7), the Hermite expansion in Eq. (2) can be cast into the following form:

$$\begin{aligned} f(\Delta \mathbf{r}) = & \frac{1}{\sqrt{(2\pi)^N}} e^{-\sum_i \Delta r_i^2/2} \left[ 1 + \sum_i \sum_{\nu=3}^{\infty} \frac{1}{\nu!} \langle H_\nu(\Delta r_i) \rangle H_\nu(\Delta r_i) \right. \\ & \left. + \sum_{i \neq j} \sum_{\nu=3}^{\infty} \frac{1}{\nu!} \sum_{p=1}^{\nu-1} \binom{\nu}{p} \langle H_p(\Delta r_i) H_{\nu-p}(\Delta r_j) \rangle H_p(\Delta r_i) H_{\nu-p}(\Delta r_j) + \sum_{i \neq j \neq k} \dots \right] \end{aligned} \quad (8)$$

The first term in Eq. (9) corresponds to a purely harmonic model given by the Gaussian probability distribution

$$f_0(\Delta \mathbf{r}) = \frac{1}{\sqrt{(2\pi)^N}} e^{-\sum_i \Delta r_i^2/2} . \quad (9)$$

This is the starting point for most of the past studies on protein fluctuations [10]. The next term in Eq. (9) is appreciable when the fluctuations are anharmonic, but gives no information about mode-coupling. In fact, the most general mode-amplitude distribution of an anharmonic model composed of decoupled modes is

$$\begin{aligned} f_1(\Delta \mathbf{r}) = & \frac{1}{\sqrt{(2\pi)^N}} e^{-\sum_i \Delta r_i^2/2} \times \\ & \prod_i \left[ 1 + \sum_{\nu=3}^{\infty} \frac{1}{\nu!} \langle H_\nu(\Delta r_i) \rangle H_\nu(\Delta r_i) \right] \end{aligned} \quad (10)$$

The approximation to the true distribution given in Eq. (10) is named  $f_1$  in order to remind the reader that it qualitatively improves on the Gaussian approximation  $f_0$  of Eq. (9). The difference between the full pdf given in Eq. (8) and the approximation  $f_1$  is the mode-coupling corrections such as

$$\langle H_p(\Delta r_i) H_{\nu-p}(\Delta r_j) \rangle - \langle H_p(\Delta r_i) \rangle \langle H_{\nu-p}(\Delta r_j) \rangle \neq 0$$

and higher order cumulants. Note that, marginal distributions are transparent to such corrections



**Figure 2.** Time plots of the slowest 1<sup>st</sup>, 5<sup>th</sup>, 10<sup>th</sup>, and 50<sup>th</sup> modes between timesteps 8000-8500.

$$f(\Delta r_i) \equiv \int_0^\infty \prod_{j \neq i} d\Delta r_j f(\Delta \mathbf{r}) \quad (11)$$

as a merit of the orthogonality relation in Eq. (5). Therefore, even if the marginal distributions are reproduced to good accuracy, the multidimensional free-energy landscape of the protein may still be very different from that implied by a model based on Eq. (10). We demonstrate below that this is the case for the protein Crambin. To this end, we improve the approximation in Eq. (10) one step further and approximate  $f(\Delta \mathbf{r})$  by

$$f_2(\Delta \mathbf{r}) \equiv f(\Delta \mathbf{r}) - \sum_{i \neq j \neq k} \dots \quad (12)$$

, i.e., the part of the Hermite expansion spelled out in Eq. (9) which takes into account the mode-coupling corrections at the lowest order they appear while ignoring cubic and higher-order terms. An magnitude of the neglected terms can be estimated through other means presented at the end of our paper.

### 3. Results

#### 3.1. Crambin molecular dynamics: a test ground

Crambin (Protein Data bank code 1EJG.pdb) was selected as a test ground since it is a relatively small protein and its dynamics is widely studied. [11, 12, 13] The 46 residue Crambin consists of 657 atoms. Taking only the alpha carbons into account a set of 138 modes were obtained, six of which have a zero eigenvalue corresponding to the translation of the center of mass and three global rotational degrees of freedom around it.

All molecular dynamics simulations were performed for an N,P,T ensemble in explicit solvent (water) at 310 K using NAMD 2.5 package with CHARMM27 force field. The protein was solvated in a waterbox of 15 Å cushion and periodic boundary conditions were applied. Ions were added in order to represent a more typical biological environment. Langevin dynamics was used to control the system's temperature and

pressure. All atoms were coupled to the heat bath of temperature of 310 K. A time step of 1fs was used. Nonbonded and electrostatic forces were evaluated at each time step. In order to keep all degrees of freedom no rigid bonds were used. All structures were translated so that their centers of mass are positioned at the origin and rotated to yield the best mass weighted RMSD agreement with the initial structure [5].

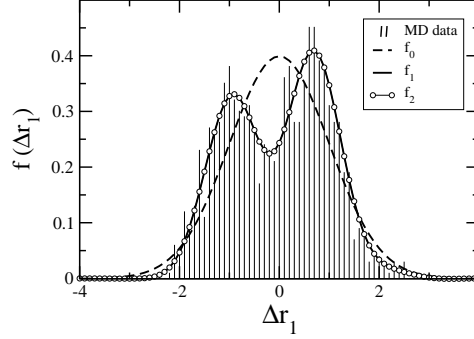


**Figure 3.** A comparison of  $f_0$  and  $f_1$  and  $f_2$  on the normalized histogram of the slowest mode. Note that  $f_1$  and  $f_2$  give the same marginal mode probabilities.

The full dataset consists of 8967 snapshots of 132 modes taken at 0.1 ps intervals. To prevent overfitting, every 9-th snapshot (a total of 996) was reserved as the test set and the rest (7971 snapshots) were used as the training set. Fig. 2 gives the time plots of a few of the sample modes.

### 3.2. Entropy estimation

In order to compare the quality of the three models  $f_0$ ,  $f_1$  and  $f_2$  (given respectively by Eqs. (9, 10, and 12)), we use the average log likelihood of the snapshots in the test data, given the parameters optimized for the training data. Eq. (13) defines the average log likelihood of the data.  $\Delta \mathbf{r}^{(i)}$  denotes the  $i$ -th snapshot and  $\mathcal{N}$  is the number of snapshots.

$$\begin{aligned} \langle \log f(\Delta \mathbf{r}) \rangle &= \int f(\Delta \mathbf{r}) \log f(\Delta \mathbf{r}) d\Delta \mathbf{r} \\ &\approx \frac{1}{\mathcal{N}} \sum_{i=1}^{\mathcal{N}} \log f(\Delta \mathbf{r}^{(i)}) \end{aligned} \quad (13)$$

From the definition of the log likelihood given in Eq. (13) it immediately follows that the entropy,  $S$ , can be estimated as  $S/k_B = -\langle \log f(\Delta \mathbf{r}) \rangle$  where  $k_B$  is the Boltzmann constant. The average log likelihood based on  $f_0$  is -187.5 per snapshot, corresponding to 115.5 kcal/mol contribution to the free energy. The latter is obtained as  $TS = -RT \langle \log f(\Delta \mathbf{r}) \rangle$ ,  $R = 1.986$  cal/mol,  $T = 310$  K.

Fig. (3) compares the  $f_0$  and  $f_1$  distributions for the slowest mode, obtained from the test data. The anharmonicity of the dynamics is clear and is well represented by  $f_1$ . The free energy equivalent of the  $f_1$  entropy is 115.1 kcal/mol which is only 0.4% less than that of  $f_0$ .

### 3.3. Mode-coupling corrections

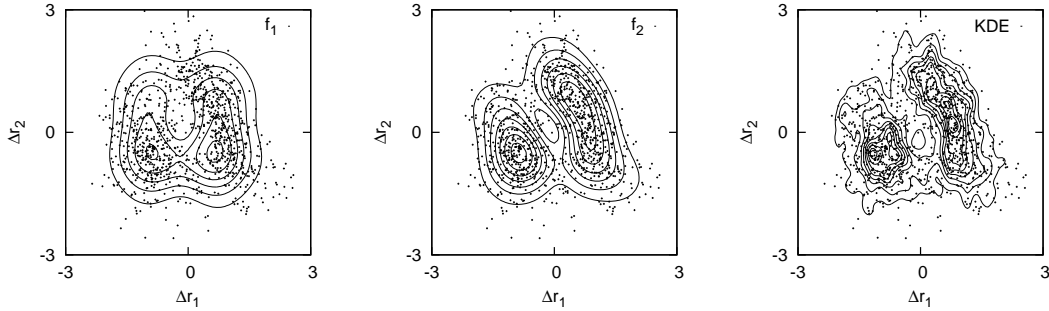


**Figure 4.** A comparison of  $f_1$ ,  $f_2$  and KDE against a scatter plot of the two slowest modes.

The  $f_2$  approximation in Eq. (8) introduces pairwise interactions between modes. Note that, the correction due to the mode-coupling terms included in  $f_2$  is invisible at the level of the marginal distributions, such as in Fig. (3). Therefore we compare in the first two panels of Fig. 4 the contour plots of  $f_1$  and  $f_2$  distributions with the scatter plot of the two slowest modes. The free energy landscape of the protein is captured visibly better by  $f_2$  when compared to  $f_1$ . The contribution at the level of  $f_2$  to free energy equivalent of entropy is 110.9 kcal/mol. This results in a correction of  $\approx -4.6$  kcal/mol to the free energy *solely due to mode-coupling*.

### 3.4. Higher-order coupling

To quantify the effects of phenomena beyond pairwise interactions, we further used non-parametric kernel density estimation (KDE) procedure to model the probability density of the training set. In this approach, one fits the data using second-order Gaussian kernels with fixed bandwidths optimized by likelihood cross validation. We used the “npudensbw” and “npudens” procedures from the “np” package for the “R” statistical computing environment [14].

In Fig. 4, the results of KDE are presented in the third panel. These results are representative of all orders of contributions to anharmonicity and mode coupling and may be used to obtain a reasonable upper bound on the impact of mode-coupling on protein energetics. The free energy equivalent of the entropy calculated by the KDE is 108.4 kcal/mol. This shows that the total reduction in entropy due to anharmonicities and coupling relative to Gaussian is 7.1 kcal/mol, or 6.1% for Crambin.

## 4. Conclusion

The probability distributions of residue fluctuations obtained by the Hermite series expansion and the KDE give consistent measures of the fluctuational entropy of the protein Crambin in its native state. The Gaussian approximation  $f_0$  gives a value of  $TS = 115.5$  kcal/mol. Introduction of anharmonicities in the absence of mode coupling reduces the entropy to  $TS = 115.1$  kcal/mol. Inclusion of second order mode coupling further reduces the entropy to  $TS = 110.9$  kcal/mol. The KDE, which takes all orders of correlations and mode coupling into account yields an entropy of  $TS = 108.4$  kcal/mol. In conclusion, we find that the effect of anharmonicity and correlations on the entropy is about 6% as determined from the difference between the Gaussian and the KDE approximations. The Hermite expansion of the configurational p.d.f. suggests that the correlations (i.e., mode-coupling) account for a large portion of this correction. In a strict sense, 6% is a lower bound on the best estimate one can obtain from the given data - although, presumably not too far from it in view of the nonparametric nature of the KDE method. Finally, in spite of their relatively small weight, we see that both corrections to the Gaussian approximation strongly modify the shape of the free-energy landscape of the protein in the vicinity of its native state.

## References

- [1] I. Bahar, A.R. Atilgan, and B. Erman. Direct evaluation of thermal fluctuations in proteins using a single-parameter harmonic potential. *Folding and Design*, 2(3):173–181, 1997.
- [2] AR Atilgan, SR Durell, RL Jernigan, MC Demirel, O. Keskin, and I. Bahar. Anisotropy of fluctuation dynamics of proteins with an elastic network model. *Biophys. J.*, 80(1):505–515, 2001.
- [3] S. Hayward, A. Kitao, and N. Go. Harmonic and anharmonic aspects in the dynamics of BPTI: a normal mode analysis and principal component analysis. *Protein Science*, 3(6):936, 1994.
- [4] F. Pontiggia, G. Colombo, C. Micheletti, and H. Orland. Anharmonicity and self-similarity of the free energy landscape of protein G. *Phys. Rev. Lett.*, 98(4):48102, 2007.
- [5] O.N. Yogurtcu, M. Gur, and B. Erman. Statistical thermodynamics of residue fluctuations in native proteins. *J. Chem. Phys.*, 130(9), 2009.
- [6] K. Moritsugu, O. Miyashita, and A. Kidera. Vibrational energy transfer in a protein molecule. *Phys. Rev. Lett.*, 85(18):3970–3973, 2000.
- [7] DM Leitner. Energy flow in proteins. *Annual Review of Physical Chemistry*, 59:233–259, 2008.
- [8] A.E. García. Large-amplitude nonlinear motions in proteins. *Phys. Rev. Lett.*, 68(17):2696–2699, 1992.
- [9] PJ Flory and DY Yoon. Moments and distribution functions for polymer chains of finite length. I. Theory. *J. Chem. Phys.*, 61:5358–5365, 1974.
- [10] Q. Cui and I. Bahar. *Normal mode analysis: theory and applications to biological and chemical systems*. CRC Press, 2006.
- [11] M.M. Teeter and D.A. Case. Harmonic and quasiharmonic descriptions of crambin. *J. Phys. Chem.*, 94(21):8091–8097, 1990.
- [12] M. Levitt, C. Sander, and P.S. Stern. Protein normal-mode dynamics: trypsin inhibitor, crambin, ribonuclease and lysozyme. *J. Mol. Biol.*, 181(3):423–447, 1985.
- [13] O.F. Lange and H. Grubmüller. Can principal components yield a dimension reduced description of protein dynamics on long time scales? *J. Phys. Chem. B*, 110(45):22842–22852, 2006.



- [14] T. Hayfield and J.S. Racine. Nonparametric econometrics: The np package. *Journal of Statistical Software*, 27(5):1–32, 2008.